The Central Executioner of Apoptosis: Multiple Connections between Protease Activation and Mitochondria in Fas/APO-1/CD95- and Ceramide-induced Apoptosis

By Santos A. Susin,* Naoufal Zamzami,* Maria Castedo,* Eric Daugas,* Hong-Gang Wang,‡ Stephan Geley,§ Florence Fassy,‖ John C. Reed,‡ and Guido Kroemer*

*From the *Centre National de la Recherche Scientifique-UPR420, B.P.8, F-94801 Villejuif, France; ‡The Burnham Institute, La Jolla, California 92037; §Institute for General and Experimental Pathology of the University of Innsbruck, A-6020 Innsbruck, Austria; and ‖Division Santé, Domain Immunologie, ROUSSEL UCLAF, F-93235 Romainville, France*

Summary

According to current understanding, cytoplasmic events including activation of protease cascades and mitochondrial permeability transition (PT) participate in the control of nuclear apoptosis. However, the relationship between protease activation and PT has remained elusive. When apoptosis is induced by cross-linking of the Fas/APO-1/CD95 receptor, activation of interleukin-1β converting enzyme (ICE; caspase 1) or ICE-like enzymes precedes the disruption of the mitochondrial inner transmembrane potential ($\Delta\Psi_m$). In contrast, cytosolic CPP32/Yama/Apopain/caspase 3 activation, plasma membrane phosphatidyl serine exposure, and nuclear apoptosis only occur in cells in which the $\Delta\Psi_m$ is fully disrupted. Transfection with the cowpox protease inhibitor *crmA* or culture in the presence of the synthetic ICE-specific inhibitor Ac-YVAD.cmk both prevent the $\Delta\Psi_m$ collapse and subsequent apoptosis. Cytosols from anti-Fas–treated human lymphoma cells accumulate an activity that induces PT in isolated mitochondria in vitro and that is neutralized by crmA or Ac-YVAD.cmk. Recombinant purified ICE suffices to cause isolated mitochondria to undergo PT-like large amplitude swelling and to disrupt their $\Delta\Psi_m$. In addition, ICE-treated mitochondria release an apoptosis-inducing factor (AIF) that induces apoptotic changes (chromatin condensation and oligonucleosomal DNA fragmentation) in isolated nuclei in vitro. AIF is a protease (or protease activator) that can be inhibited by the broad spectrum apoptosis inhibitor Z-VAD.fmk and that causes the proteolytical activation of CPP32. Although Bcl-2 is a highly efficient inhibitor of mitochondrial alterations (large amplitude swelling + $\Delta\Psi_m$ collapse + release of AIF) induced by prooxidants or cytosols from ceramide-treated cells, it has no effect on the ICE-induced mitochondrial PT and AIF release. These data connect a protease activation pathway with the mitochondrial phase of apoptosis regulation. In addition, they provide a plausible explanation of why Bcl-2 fails to interfere with Fas-triggered apoptosis in most cell types, yet prevents ceramide- and prooxidant-induced apoptosis.

It is currently assumed that the apoptotic process can be divided into at least three functionally distinct phases (1–5). During the heterogeneous initiation phase, cells receive the death-inducing stimulus via certain receptors such as the TNF receptor or Fas/APO-1/CD95, shortage of obligatory growth factors, oxygen or metabolic supply, or subnecrotic physical and chemical damage. The biochemical events participating in the initiation phase constitute "private" pathways in the sense that they depend on the lethal stimulus. It is only during the subsequent phases that these initiating events are translated into a regular common pattern of metabolic reactions. The common pathway can be subdivided into an initial effector phase, during which the "central executioner of apoptosis" is still subject to regulatory mechanisms, and a later degradation phase, beyond the "point of no return", during which catabolic enzymes become activated in an irreversible fashion. During the degradation phase the morphology and characteristic biochemistry of apoptosis (e.g., step-wise DNA fragmentation, and specific proteolysis of cytoplasmic and nuclear substrates) become manifest (1–5).

Two nonexclusive mechanisms have been proposed to intervene as central executioners of the apoptotic effector phase. On one hand, it appears that apoptosis is associated

 J. Exp. Med. © The Rockefeller University Press • 0022-1007/97/07/25/13 $2.00
Volume 186, Number 1, July 7, 1997 25–37

with the critical activation of a family of specific proteases that include interleukin-1β converting enzyme (ICE[1]/caspase 1), CPP32 (Yama/Apopain/caspase 3), and other proteases homologous to the *Caenorhabditis elegans* protein Ced-3 (1–3, 5). On the other hand, the disruption of the mitochondrial inner transmembrane potential ($\Delta\Psi_m$) marks a point of no return for the apoptotic cascade (6). Moreover, mitochondria that undergo permeability transition (PT) or products derived from these organelles induce chromatin condensation and DNA fragmentation in cell-free systems of apoptosis (7–11).

Two mitochondrial proapoptotic factors have been purified: (*a*) the 15-kD cytochrome *c* protein, which acts together with cytosolic factors to induce nuclear apoptosis (10), and (*b*) a ~50-kD protease that by itself suffices to cause nuclear apoptosis (11). We have recently shown that mitochondria release such a ~50-kD apoptogenic protein (apoptosis-inducing factor, AIF) when they undergo PT (9, 11), a phenomenon that accounts for $\Delta\Psi_m$ disruption in intact cells (9, 12, 13) and that is accompanied by the release of cytochrome *c* (14). The oncoprotein Bcl-2 is an inhibitor of PT induced in isolated mitochondria (9, 11), anucleate cytoplasts (15), and cells (12), underscoring the idea that PT may indeed constitute a central checkpoint of the apoptotic cascade. Pharmacological inhibition of PT by mitochondrion-targeted drugs can inhibit all cytoplasmic and nuclear manifestations of apoptosis (9, 13, 15), suggesting that PT is a rate-limiting, coordinating step of apoptosis. PT is induced by many different physiological effectors (reactive oxygen species, blockade of the respiratory chain, changes in the ATP/ADP concentration, pyrimidine nucleotide oxidation, thiol redox potentials, calcium, etc.), and thus may allow for the convergence of very different inducers of apoptosis. The multiplicity of PT induction pathways is underscored by the fact that none of the known inhibitors of PT, including Bcl-2, can block PT induction in all circumstances (9, 11, 16).

The hierarchical relationship between protease activation and mitochondrial PT appears complex. The available data suggest three levels of interaction between proteases and PT. First, proteases may act upstream of PT. Thus, inhibitors of serine proteases such as *N*-tosyl-l-lysyl chloromethylketone and degenerate tripeptidic inhibitors of ICE-like proteases such as *N*-benzyloxycarbonyl-Val-Ala-Asp.fluoromethylketone (Z-VAD.fmk) prevent or retard the glucocorticoid-induced $\Delta\Psi_m$ disruption and subsequent apoptosis in thymocytes (13). Second, PT may be regulated directly by mitochondrial proteases. Thus, calcium- and prooxidant-induced PT may involve the action of a mitochondrial calpain-like protease (17). Third, proteases may also act downstream of PT. We have recently shown that the apoptogenic protein (AIF) released from mitochondria undergoing PT possesses a proteolytic activity that is also inhibited by Z-VAD.fmk (11).

Prompted by these findings, we have studied the possible impact of proteases on PT in one prototypic model of apoptosis, namely apoptosis induced via ligation of the Fas surface receptor. Fas-mediated cell death is thought to contribute to the maintenance of immune homeostasis, to immune surveillance of mutating or virus-infected cells, as well as to the pathological depletion of $CD4^+$ lymphocytes in AIDS (18, 19). It involves the activation of specific proteases, namely an ICE-like protease associated with the Fas receptor complex (FLICE/Mach-1/Mch-5/caspase 8; references 20, 21), ICE (caspase 1; references 22–24), and CPP32 (caspase 3; reference 25). Fas-triggered apoptosis is unique in the sense that it constitutes the only known apoptosis induction pathway that relies on the specific intervention of ICE (22–24). In addition, Fas-induced apoptosis is not inhibited by Bcl-2, at least in some cell types (26–28). This has lead to the speculation that Fas and Bcl-2 would regulate different pathways of apoptosis induction (26–28). Thus, Fas could trigger an apoptotic pathway that bypasses the putative Bcl-2/PT checkpoint of the apoptotic effector phase. Alternatively, it could induce PT in a fashion that is not controlled by Bcl-2.

In this work, we discriminate between these possibilities and present evidence indicating that, during Fas-induced apoptosis, ICE functions as a direct inducer of mitochondrial PT. Although Bcl-2 efficiently inhibits mitochondrial PT induced by a variety of different stimuli including prooxidants, it completely fails to interfere with ICE-induced signs of mitochondrial PT including $\Delta\Psi_m$ disruption and release of AIF. We show that AIF possesses unique biological properties. In addition to its direct apoptotic effect on isolated nuclei in a cell-free, cytosol-free system, AIF is itself an inducer of PT, and thus may be involved in a positive amplification loop disrupting mitochondrial function. Moreover, AIF proteolytically activates CPP32, one of the signature proteases of mammalian cell death. These findings underscore the implication of mitochondria in the apoptotic effector phase, provide multiple links between proteases and mitochondrial regulation, and explain the limited apoptosis-inhibitory effect of Bcl-2. Moreover, our data suggest a scenario according to which ICE (or ICE-like proteases), mitochondrial AIF, and CPP32 are sequentially activated and participate in the induction, effector, and degradation phases of apoptosis, respectively.

Materials and Methods

Cell Lines and Culture Conditions. Human CEM-C7.H2 lymphoma cells were transfected with a PHD1.2 *crmA* cDNA (1.46 kb) cloned in the sense orientation into a β-actin STneo B vector (crmA cells) or a vector-only control (Neo). Three different clones hyperexpressing crmA at the protein level yielded similar functional results. Results are shown for the C7.H2/D1.2/2E8 clone. Alternatively, CEM-C7.H2 cells were transfected with pEF-tTA 2A10, a doxycyclin-inhibitable transactivator (tTa) and super-transfected with a tTa-repressed *bcl-2* construct in a tk-Hyg

[1]*Abbreviations used in this paper:* $\Delta\Psi_m$, mitochondrial transmembrane potential; AIF, apoptosis-inducing factor; CFS, cell-free system; CMXRos, cholormethyl-X-rosamine; ICE, interleukin 1β converting enzyme; mClCCP, carbonyl cyanide m-chlorophenylhydrazone; PT, permeability transition; *t*-BHP, ter-butylhydroperoxide.

selection vector (pUGD10-3 Bcl-2 tkHyg; reference 29; results are shown for one out of two clones yielding similar data). Bcl-2 expression was repressed by culture on doxycycline (10 ng/ml, 48 h), as described (30). Apoptosis was induced by stimulation of 1–5 × 10^6 cells/ml with the Fas–cross-linking IgM monoclonal antibody CH-11 (500 ng/ml; Immunotech, Marseille, France) in the presence or absence of the membrane-permeant–specific inhibitor of ICE, Ac-YVAD.cmk (100 μM; Bachem, Basel, Switzerland), or alternatively with C_2 ceramide (50 μM; Sigma Chemical Co., St. Louis, MO).

Cytofluorometric Determinations of Apoptosis-associated Alterations in Whole Cells. To evaluate the $\Delta\Psi_m$, cells (10^6/ml) were incubated with the cationic lipophilic dye chloromethyl-X-rosamine (CMXRos; 150 nM; Molecular Probes, Inc., Eugene, OR; reference 15). As a control, cells were simultaneously treated with the uncoupling agent carbonyl cyanide m-chlorophenylhydrazone (mClCCP; 50 μM; Sigma Chemical Co.). CMXRos incorporates into mitochondria driven by the $\Delta\Psi_m$ (15) and reacts with thiol residues to form covalent aldehyde-fixable thiol ester bonds (31). After fixation (4% paraformaldehyde in PBS for 15 min at room temperature), cells were washed and stained for the detection of chromatinolysis using the TUNEL method, as described (31). In one series of experiments, cells were stained with the potential-sensitive dye $DiOC_6(3)$ (15 min, 37°C, 40 nM) together with a biotin–Annexin V conjugate (50 × dilution; revealed by streptavidine-phycoerythrine at 5 μg/ml, following the manufacturer's protocol; Boehringer Mannheim GmbH, Mannheim, Germany), followed by sorting of $DiOC_6(3)^{low}$ Annexin V^+, $DiOC_6$ (3) Annexin V^- and $DiOC_6(3)^{high}$ Annexin V^+ cells on an Elite cytofluorometer (Coulter Corp., Miami, FL), as described (6, 15).

Preparation of Cytosols and Determination of the Activity of ICE-like Proteases. 100 μl cytosols (10^7 cells/100 μl in cell-free system [CFS] buffer [220 mM mannitol, 68 mM sucrose, 2 mM NaCl, 2.5 mM PO_4H_2K, 0.5 mM EGTA, 2 mM $MgCl_2$, 5 mM pyruvate, 0.1 mM PMSF, 1 mM dithiotreitol, 10 mM Hepes-NaOH]) and pH 7.4 buffer (supplemented with additional protease inhibitors: 1 μg/ml leupeptin, 1 μg/ml pepstatin A, 50 μg/ml antipain, 10 μg/ml chymopapain) were prepared by five freeze/thaw cycles in liquid nitrogen, followed by centrifugation (1.5 × 10^5 *g*, 4°C, 1 h) as described (32). The protein concentration in the supernatant was determined by the Bradford assay (Bio Rad Labs., Hercules, CA). ICE activity was measured using a fluorogenic substrate containing the cleavage site YVAD, 4-(4′-deimethylaminophenylazo) benzoic-YVADAPV-5-(-2-aminoethyl-amino) naphtalene-1-sulfonic acid (Bachem), as described (22), using a spectrofluorometer (Kontron SFM 25; Kontron AG, Zurich, Switzerland). The capacity of cytosols or purified recombinant human CPP32 activity to cleave the CPP32 recognition site DEVD was determined using Ac-DEVD-amino-4-methylcoumarin (Bachem) as fluorogenic substrate (33).

Preparation of Organelles. Mitochondria were isolated from BALB/c hepatocytes (6–8 wk, female) or from different CEM-C7.H2 lines. Mitochondria were purified on a Percoll® (Pharmacia, Uppsala, Sweden) gradient (34) and were stored on ice in CFS buffer for up to 4 h. Mitochondria were washed and resuspended in CFS supplemented with 2 mM ATP. Nuclei from HeLa cells were purified on a sucrose gradient and conserved in 50% glycerol (Sigma Chemical Co.) in HeLa nuclei buffer at −20°C for a maximum of 15 d, as described (35).

Purification of the Mitochondrial AIF. Purified hepatocyte mitochondria were treated with atractyloside (5 mM; Atr; Sigma Chemical Co.) to induce PT and liberation of AIF (9, 11). Supernatants (150,000 *g*, 1 h, 4°C) from these mitochondria were concentrated on Centricon 10 membranes (≥10 kD; Amicon, Beverly, MA) and then injected into a FPLC column (MonoQ (HR5/5); Pharmacia) preequilibrated with protein-free CFS buffer (see below). Elution was performed on a linear gradient from 0 to 250 mM NaCl at 0.5 ml/min over 30 min, followed by elution at 1 M NaCl thereafter. All fractionation steps were carried out at 4°C to avoid loss of biological AIF activity. The active fraction (eluting at 110 mM NaCl; reference 11) was dialyzed against protein-free CFS buffer (4°C, overnight, 5,000× excess of CFS buffer), concentrated on Centricon 10 membranes, adjusted to a concentration of 30 μg/ml, and aliquoted to be snap frozen in liquid nitrogen and stored at −80°C.

Determination of Mitochondrial PT. For the induction of PT, mitochondria from different cell lines were incubated with cytosolic extracts from αFas–treated cells (standard dose of 30 μg protein/ml), purified recombinant ICE (50 μg/ml), the prooxidant ter-butylhydroperoxide (*t*-BHP; 30 μM), atractyloside (5 mM; Sigma Chemical Co.), the protonophore mClCCP (100 μl; Sigma Chemical Co.), bongkrekic acid (50 μM; provided by Dr. Duine, Delf University, Delf, The Netherlands), monochlorobiman (30 μM; Sigma Chemical Co.), and/or the calpain inhibitor *N*-benzyloxycarbonyl-l-leucyl-l-leucyl-l-tyrosine diazomethylketone (100 μM; Molecular Probes Inc., reference 9). Recombinant ICE was produced following standard procedures (36) and was allowed to partially (≤5%) autoactivate by incubation at 20°C for 2 h, followed by storage on ice for a maximum of 4 h. Two different consequences of PT were assessed: (*a*) mitochondrial large amplitude swelling and (*b*) collapse of the $\Delta\Psi_m$. For determination of swelling, mitochondria were washed and resuspended in CFS buffer supplemented with 2 mM ATP at a concentration of 100 μg mitochondrial protein/10 μl buffer, followed by addition of 90 μM CFS containing 2 mM ATP and recording of adsorption at 540 nm in a spectrophotometer (DU 7400; Beckman Instrs., Carlsbad, CA), as described (9). After stabilization of the adsorption during a minimum interval of 30 s, the indicated substance was added in a volume of 5 μl. The loss of absorption induced by 5 mM atrectyloside within 5 min was considered 100% of the large amplitude swelling, as described (9). The $\Delta\Psi_m$ was measured using $DiOC_6$ (3) (40 nM, 15 min at 37°C; Molecular Probes Inc.), after having added the indicated PT inducer (30 min, room temperature). Mitochondria were analyzed in an Elite cytofluorometer (Coulter Corp.). All $\Delta\Psi_m$ determinations were performed at least three times in each experiment.

Cell-free System of Apoptosis. Nuclei from mouse liver cells were purified on a sucrose gradient (35), washed two times (1,000 *g*, 10 min, 4°C), and resuspended in CFS buffer. In standard conditions, nuclei (10^3 nuclei/μl) were cultured in the presence of mitochondrial preparations for 90 min at 37°C. Nuclei were stained with propidium iodide (10 μg/ml; Sigma Chemical Co.) and the lipophilic dye 5-methyl-bodipy-3-dodecanoic acid (100 nM; Molecular Probes Inc., reference 37), followed by cytofluorometric analysis in an analyzer (EPICS Profile II Analyzer; Coulter Corp.). Only membrane surrounded (5-methyl-bodipy-3-dodecanoic acid-labeled) particles were gated. A good correlation between the frequency of nuclei exhibiting chromatin condensation with 4′-6-diamidino-2-phenylindole dihydrochloride (10 μM; Molecular Probes, Leiden, The Netherlands; reference 38) and hypoploidy with PI was obtained (Susin, S.A., and G. Kroemer, manuscript in preparation). DNA fragmentation was determined by horizontal agarose gel electrophoresis and ethidium bromide staining as described (9). Electron microscopy of osmium tetroxyde-fixed nuclei was performed as described (13).

Expression of Human CPP32 and Generation of a Specific Antiserum. A cDNA encoding human CPP32 was generated by PCR using the plasmid pKSII-CPP32 (gift from Guy Salvesen, Burnham Institute, La Jolla, CA) as a template and the primers 5′-GGAATTCCATATGGAGAACACTGAAAACTCAGTG-3′ (forward) and 5′-CCGCTCGAGGTGATAAAAATAGAGTTCTTTTG-3′ (reverse). After digestion with XhoI and NdeI, this PCR-generated cDNA was subcloned into pET21b at the NdeI/XhoI sites to produce CPP32 protein with six histidine resides at its COOH terminus. Recombinant purified CPP32 was purified as described (39). New Zealand white female rabbits were injected subcutaneously with 200 μg of purified CPP32-His_6 fusion protein mixed (1:1 vol/vol) with Freund's complete adjuvant and then boosted seven times with 200 μg of protein in Freund's incomplete adjuvant before collecting blood and obtaining immune serum.

Western Blot Analysis. AIF-mediated cleavage of nuclear substrates was determined by the comparative analysis of SDS-PAGE of HeLa nuclei (5×10^6/lane) cultured in the presence or absence of supernatant from Atr-treated mitochondria (10 μg protein/ml, 90 min, 37°C) in the presence or absence of Z-VAD.fmk, as described (11). Western blots of these nuclei were tested for degradation of poly (ADP-ribose) polymerase (PARP) using the monoclonal antibody C2-10 (purchased from Guy Poirier, Montreal University, Canada; reference 38). Cleavage of CPP32 in cells (8×10^5 cells/lane) or in vitro (10 ng recombinant CPP32+ 10 μg protein of mitochondrial supernatant in 50 μl CFS buffer ± 100 μM Z-VAD.fmk, 15 min at 37°C) was determined by using a polyclonal rabbit antiserum recognizing both CPP32 and the p17 fragment of proteolytically activated CPP32 (39). Enzymatic activation of CPP32 (100 ng CPP32 + variable amounts of mitochondrial supernatant in 100 μl CFS buffer ± 100 μM Z-VAD.fmk, 15 min at 37°C) was detected by adding 1 μM Ac-DEVD-amino-4-methylcoumarin (30 min, 37°C), as described above. In one control experiment, Z-VAD.fmk (100 μM) was added together with Ac-DEVD-amino-4-methylcoumarin.

Results

Fas Cross-linking Provokes Sequential Activation of ICE-like Proteases, $\Delta\Psi_m$ Disruption plus Activation of CPP32, and Nuclear Apoptosis. Human CEM-C7.H2 lymphoma cells can be induced to undergo apoptosis by cross-linking of Fas. As shown in Fig. 1 *A*, cells manifest a rapid activation of protease(s) capable of cleaving a fluorogenic substrate containing the tetrapeptide YVAD. As described (22, 25), activation of ICE-like proteases is a rapid process that peaks 15–30 min after Fas cross-linking. It thus precedes the Fas-induced $\Delta\Psi_m$ disruption, as quantified by means of the $\Delta\Psi_m$-sensitive dye CMXRos. This $\Delta\Psi_m$ collapse affects only a minor fraction of the cells beginning at 30 min after Fas ligation. An important fraction of cells (~ 40%) exhibits a disrupted $\Delta\Psi_m$ about 2 h after Fas cross-linking, when DEVDase activity is also significantly augmented. To further investigate the relationship between Fas-induced $\Delta\Psi_m$ disruption and activation of CPP32, CEM-C7.H2 cells were stimulated during 2 h by Fas cross-linking, followed by staining with the $\Delta\Psi_m$-sensitive dye $DiOC_6(3)$ as well as Annexin V (which measures the aberrant phosphatidyl serine exposure on the outer plasma membrane leaflet) and cytofluorometric purification of cells with a still normal $\Delta\Psi_m$ ($DiOC_6(3)^{high}$) as well as cells with a disrupted $\Delta\Psi_m$ ($DiOC_6(3)^{low}$) that are either in an early stage of the apoptotic process (Annexin V^-) or in an advanced stage (Annexin V^+) (Fig. 1 *B*). Only $\Delta\Psi_m{}^{low}$ cells have cleaved the CPP32 precursor to yield CPP32 fragments (p21 and p17) and exhibit DEVDase activity (Fig. 1 *B*). This is observed for both $\Delta\Psi_m{}^{low}$ Annexin V^- and $\Delta\Psi_m{}^{low}$ Annexin V^+ cells, indicating that CPP32/DEVDase activation occurs concomitant with (or shortly after) the $\Delta\Psi_m$ disruption. In contrast, $\Delta\Psi_m{}^{high}$ cells behave like unstimulated control cells and lack any detectable CPP32 cleavage or DEVDase activation (Fig. 1 *B*). Thus, CPP32 is only activated in cells whose $\Delta\Psi_m$ is disrupted. Similar results have been obtained in other models of apoptosis induction, including ceramide-induced cell death (not shown). As in other models of apoptosis induction (4, 6, 9, 12, 31), the Fas-induced $\Delta\Psi_m$ collapse precedes nuclear chromatinolysis as identified with the TUNEL technique (Fig. 1 *A*). Thus, cells that have disrupted their $\Delta\Psi_m$ ($CMXRos^{low}$ cells) can be subdivided into $TUNEL^+$ and $TUNEL^-$ populations, whereas $TUNEL^+$ cells uniformly possess a $\Delta\Psi_m{}^{low}$ ($CMXRos^{low}$) phenotype (Fig. 1 *C*). These findings place $\Delta\Psi_m$ disruption upstream of nuclear apoptosis.

ICE-like proteases are involved in both the $\Delta\Psi_m$ disruption and chromatinolysis, because cells treated with the ICE-specific inhibitor Ac-YVAD.cmk or cells stably transfected with the ICE inhibitor crmA fail to demonstrate mitochondrial or nuclear manifestations of apoptosis in response to Fas cross-linking (Fig. 1 *C*). Thus, in Fas-induced apoptosis, ICE (or ICE-like proteases) function upstream of mitochondria. Transfection-enforced hyperexpression of Bcl-2 does not interfere with Fas-triggered apoptotic changes, although it does prevent both the $\Delta\Psi_m$ dissipation and DNA loss induced by the apoptosis-inducing second messenger ceramide (Fig. 1 *C*). This finding confirms previous observations that Bcl-2 does not prevent Fas-induced apoptosis, at least in certain experimental systems (26–28).

Cytosolic ICE-like Proteases Are Necessary to Induce Mitochondrial PT. To determine the mechanism by which activation of ICE or ICE-like proteases causes $\Delta\Psi_m$ disruption, we incubated isolated hepatocyte mitochondria with cytosolic extracts from αFas–treated cells. Cytosols from αFas-treated cells, but not cytosols from sham-treated control cells, were found to induce large amplitude swelling of isolated mitochondria (Fig. 2 *A*), a sign of PT. In addition, mitochondria treated with cytosols from αFas-treated cells manifest $\Delta\Psi_m$ disruption, another sign of PT (Fig. 2 *B*). This PT-inducing activity was maximal in cytosols obtained from cells subjected to Fas cross-linking for 30 min (not shown), coinciding with the maximum activity of ICE (-like) proteases (Fig. 1 *A*). As expected based on the results in intact cells (Fig. 1 *C*), transfection with crmA impeded the cytosolic accumulation of such a PT-inducing activity (Fig. 2). In addition, the ICE-specific inhibitor Ac-YVAD.cmk and another inhibitor of ICE, Ac-YVAD.CHO (not shown), prevented the formation of the PT-inducing activity in cytosols from αFas-treated cells. Ac-YVAD.cmk also prevented the action of cytosols that already contained the

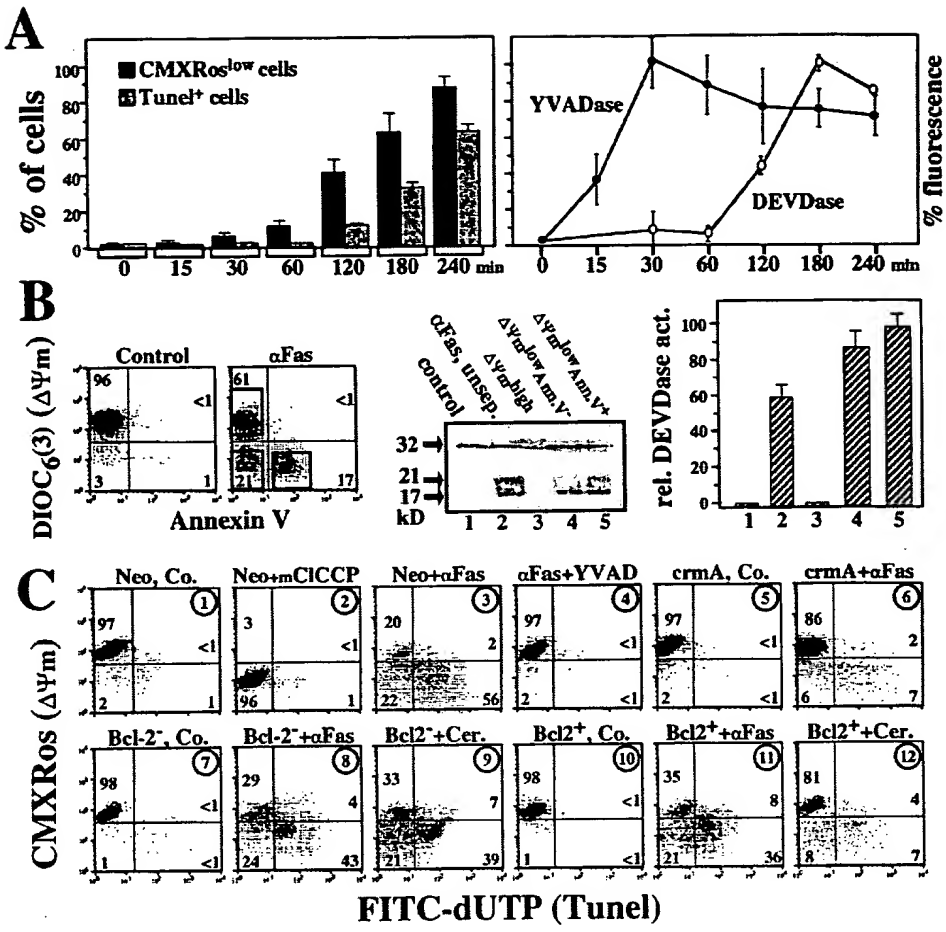

Figure 1. Chronology and cause - effect relationship between activation of ICE (or ICE-like) protease(s) and $\Delta\Psi_m$ disruption. (*A*) Chronology of the activation of ICE, $\Delta\Psi_m$ disruption, and nuclear DNA fragmentation in human CEM-C7.H2 lymphoma cells subjected to Fas cross-linking. The frequency of $\Delta\Psi_m^{low}$ cells and of cells exhibiting DNA strand breaks were determined by double staining with the potential-sensitive dye CMXRos and TdT-catalyzed FITC-dUTP incorporation (TUNEL method), as described in Materials and Methods. Note that the TUNEL$^+$ population is actually a subset of CMXRos^{low} cells (see *B*). Activation of ICE (-like) protease(s) was determined by a fluorogenic substrate containing the ICE cleavage site YVAD (*filled symbols*), the maximum activity being defined as 100%. Similarly, the activation of CPP32 (-like) protease(s) was determined by means of a fluorogenic substrate containing the cleavage site DEVD (*open symbols*). (*B*) Temporal relationship between Fas-induced $\Delta\Psi_m$ disruption and CPP32 cleavage, as well as DEVDase activation. CEM-C7.H2 cells were cultured during 120 min in the presence of anti-Fas antibody, followed by staining with the $\Delta\Psi_m$-sensitive dye $DiOC_6(3)$ plus Annexin V (revealed by phycoerythrin). Cells were then separated in the cytofluorometer into cells with a normal $\Delta\Psi_m$ ($DiOC_6(3)^{high}$ Annexin V$^-$) or cells with a $DiOC_6(3)^{low}$ Annexin V$^-$ or $DiOC^6(3)^{low}$ Annexin V$^+$ phenotype (sorting according to Windows), followed by determination of CPP32 cleavage using Western blots (lane *1*, unstimulated control cells; lane 2, nonseparated Fas-stimulated cells; lane *3*), purified $DiOC^6(3)^{high}$ cells; lane *4*, purified $DiOC_6(3)^{low}$ Annexin V$^-$ cells; lane *5*, purified $DiOC^6(3)^{low}$ Annexin V$^+$ cells, 8×10^5 cells/lane). Alternatively, cytosols from these cell populations were tested for DEVDase activity in vitro as in *A* (*C*) Determination of $\Delta\Psi_m$ disruption and DNA strand breaks in different cells. CEM-C7.H2 lymphoma cell stably transfected with a Neomycin selection vector (*Neo*) only (fluorescence displays *1–4*), with the crmA cowpox protease inhibitor (graphs *5* and *6*), or with a Bcl-2–expressing construct negatively regulated by doxycyclin (graphs *7–12*). Cells were either pretreated with doxycyclin (10 ng/ml, 48 h before starting of the experiment) to repress Bcl-2 expression (*Bcl-2$^-$*, graphs *7–9*) or left untreated (*Bcl-2$^+$*, graphs *10–12*), and then subjected to apoptosis induction with C_2 ceramide (50 μM; graphs *9* and *12*), anti-Fas (graphs *3, 4, 6, 8,* and *11*) and/or the ICE inhibitor Ac-YVAD.cmk (50 μM, all during 4 h; graph *4*), followed by double staining with CMXRos and the TUNEL method. Neo control cells were treated during 15 min with 100 μM of the protonophore mClCCP, providing a negative control for the CMXRos staining (graph *2*). Numbers indicate the percentage of cells in each quadrant. Results are representative for three independent experiments.

PT-inducing activity on mitochondria, when added to the cytosol derived from αFas-treated cells in vitro (Fig. 2). In contrast, the peptide Ac-DEVD.CHO, an inhibitor of CPP32, was ineffective (not shown). This suggests that an ICE-like protease participates in the induction of mitochondrial PT, both in cells (Fig. 1 *C*) and in a cell-free system (Fig. 2).

ICE Is Sufficient to Induce Mitochondrial PT In Vitro. In accordance with the data obtained with cytosolic extracts, recombinant purified ICE suffices to induce both large amplitude swelling and dissipation of the $\Delta\Psi_m$ in isolated mitochondria in vitro (Fig. 3, *A* and *B*). This effect of ICE is rapid (<30 s) and can be neutralized by Ac-YVAD.cmk and Ac-YVAD.CHO, but not by AcDEVD.CHO, indicating that it relies on the enzymatic activity of ICE. In contrast, Ac-YVAD.cmk does not interfere with *t*-BHP-induced PT, thus excluding that this modified tetrapeptide might prevent PT in a nonspecific fashion (Fig. 3, *A* and *B*). The use of additional inhibitors underscores the different mechanisms involved in ICE- and *t*-BHP-triggered PT. For example, cyclosporin A, bongkrekic acid, monochlorobiman (9), and the calpain inhibitor Cbz-LLT. CHN_2 (17) all inhibited the *t*-BHP- but not the ICE-induced PT in vitro (Table 1). Other proteases besides ICE, such as trypsin and proteinase K, also induce PT in isolated mitochondria (not shown), in accord with previous observations that microinjection of such proteases induces apoptosis in cells (40).

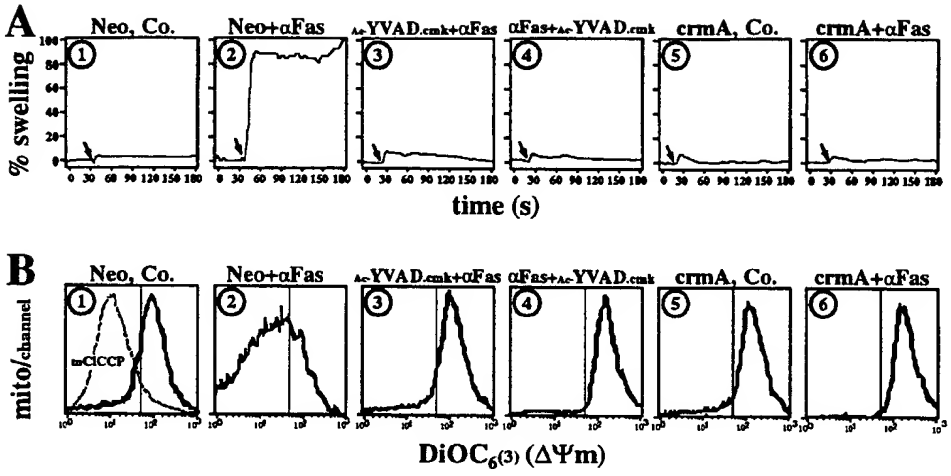

Figure 2. A cytosolic factor neutralized by ICE-specific protease inhibitors causes mitochondrial PT in vitro. Isolated hepatocyte mitochondria were exposed to cytosols (final concentration: 100 μg/ml protein) prepared from CEM-C7.H2 lymphoma cells stably transfected with a Neomycin selection vector (*Neo*) only (graphs *1–4*) or cells transfected with the crmA cowpox protease inhibitor (graphs *5* and *6*) that were either treated with anti-Fas antibody during 30 min (graphs *2–4*, *6*) or were left untreated (graphs *1* and *5*). Cytosols were tested for their capacity to induce mitochondrial swelling, 100% of swelling being defined as the loss of the OD_{540} observed 5 min after addition of 5 mM atractyloside (*A*). Arrows indicate addition of the cytosolic extract. Alternatively, the $\Delta\Psi_m$ was assessed cytofluorometrically on a per-mitochondrion basis of mitochondria treated with the indicated cytosol preparation and then stained with the potential-sensitive dye $DiOC_6(3)$ (*B*). Treatment with the protonophore mClCCP served as a negative control for $DiOC_6(3)$ staining (*dotted line*, graph *1 B*). The effect of the ICE-specific inhibitor Ac-YVAD.cmk was tested in two different ways. Ac-YVAD.cmk was either used with the cells exposed to αFas (*Ac-YVAD.cmk+αFas*, graph *3*) or, alternatively, was added to the cytosol prepared from Fas-treated cells (*αFas+Ac–YVAD.cmk*, *graph 4*).

Thus, ICE (or ICE-like) protease(s) is/are necessary and sufficient to mediate the $\Delta\Psi_m$ disruption in cells subjected to Fas ligation. The mechanism of ICE-induced PT differs from that of prooxidant-induced PT, suggesting a direct proteolytic effect of ICE on mitochondria.

ICE Causes the Mitochondrial Release of an Apoptogenic Protein, AIF. We have previously shown that PT is accompanied by the release of an apoptogenic protein that induces isolated nuclei to undergo chromatin condensation and oligonucleosomal DNA fragmentation (9, 11). Accordingly, the ICE-induced PT is accompanied by the release of such an apoptogenic protein (AIF), which causes purified HeLa nuclei to manifest DNA condensation and loss of chromosomal DNA (subdiploidy). The ICE inhibitor Ac-YVAD.cmk prevents the ICE-induced mitochondrial release of AIF (Fig. 3 *C*), yet does not interfere with the activity of AIF itself in the cell-free system of nuclear apoptosis induction (9, 11, and see below), consistent with

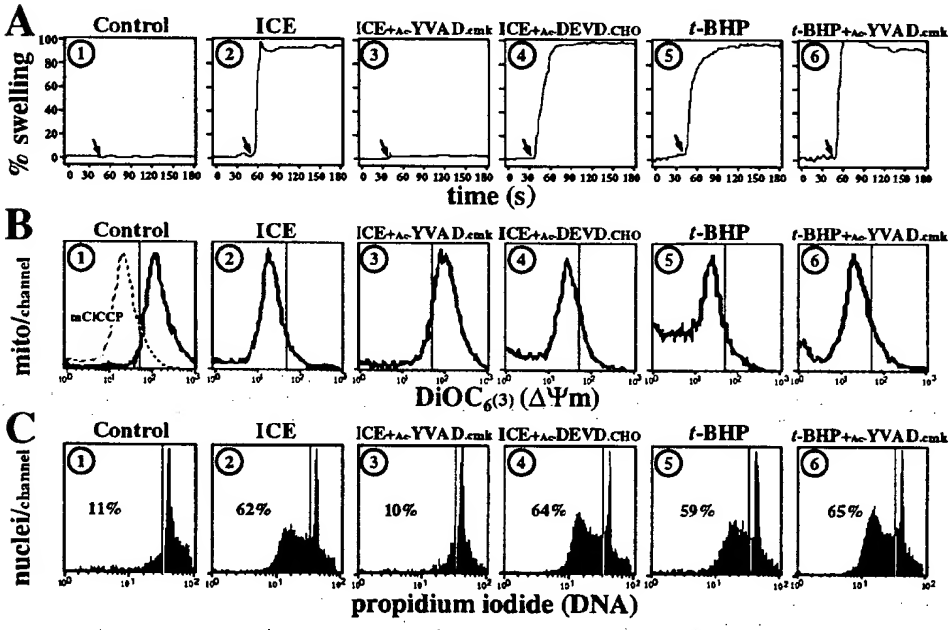

Figure 3. Recombinant purified ICE is sufficient to induce PT, as well as the release of an apoptosis-inducing factor from mitochondria. Purified liver mitochondria were treated with CFS buffer only (graph *1*), purified recombinant human ICE (graphs *2–4*), the prooxidant *t*-BHP (graphs *5* and *6*), and/or different protease inhibitors (*Ac-YVAD.cmk*, graphs *3* and *6* or *Ac-DEVD.CHO*, graph *4*). These reagents were added together to the mitochondria and the following parameters were assessed: large amplitude swelling (*A*), $\Delta\Psi_m$ ($DiOC^6(3)$ staining, 30 min after addition of the reagents) (*B*), and release of AIF (*C*). Arrows in *A* indicate addition of the indicated combination of reagents or buffer only (*Control*). The dotted line in graph *B 1* indicates the negative control of $DiOC_6(3)$ staining obtained in the presence of the $\Delta\Psi_m$-dissipating reagent mCICCP. For the determination of AIF release (*C*), mitochondria were centrifuged (1.5×10^{-5} *g*, 1 h) after 5 min of treatment, and the supernatant was incubated for 30 min with purified HeLa nuclei, followed by determination of their DNA content using the flurochrome propidium iodide, as described in Materials and Methods. Percentages detail the percentage of nuclei exhibiting an apparent subdiploidy.

Table 1. *Differential Regulation of ICE- and prooxidant-induced Mitochondrial PT*

Inhibitor of PT	Inhibitory effect on large amplitude swelling* induced by	
	t-BHP	ICE
Cyclosporin A (1 μM)	+	−
Bongkrekic acid (50 μM)	+	−
Monochlorobimane (30 μM)	+	−
Chz-LLY.CHN_2 (100 μM)	+	−
Ac-YVAD.CHO (100 μM)	−	+
Ac-DEVD.CHO (100 μM)	−	−
z-VAD.fmk (100 μM)	−	+

Positive symbols denote significant (>90%) inhibition of large amplitude swelling; negative symbols indicate <10% inhibition.
*Purified mouse hepatocyte mitochondria were tested for the large amplitude swelling induced by either ICE (50 μg/ml) and *t*-BHP (30 μM) as in Fig. 3 *A*. The indicated PT inhibitors were added 15 min before *t*-BHP or ICE, and the inhibition of large amplitude swelling was determined over a period of 5 min.

the fact that ICE by itself is insufficient to induce apoptosis in isolated nuclei (38). In conclusion, ICE-induced PT is accompanied by the release of a mitochondrial apoptogenic factor.

Bcl-2 Overexpression Prevents prooxidant-induced and Ceramide-elicited PT, and Associated Release of AIF, yet Fails to Prevent ICE-induced PT and AIF Release. As outlined in the Introduction, Bcl-2 is incapable of suppressing the Fas-induced apoptosis in a number of different models (26–28). This applies also to CEM-C7-H2 lymphoma cells (Fig. 1 *C*, see above). Since mitochondrial hyperexpression of Bcl-2 prevents the induction of PT by different substances, including prooxidants (9, 11; Fig. 4), we tested whether it would also interfere with ICE-induced PT. Mitochondria isolated from Bcl-2–transfected cells manifest large amplitude swelling when treated with recombinant ICE, exactly as do control mitochondria from cells not hyperexpressing Bcl-2. In addition, Bcl-2 hyperexpression does not prevent the mitochondrial release of AIF induced by ICE, although it does suppress the *t*-BHP–induced PT and release of AIF (Fig. 4). This dichotomy in the Bcl-2–mediated regulation of PT, inhibition of prooxidant-induced PT and failure to prevent ICE-induced PT, was observed in human CEM-C7-H2 cells transfected with tetracycline-repressable *bcl-2* construct (Fig. 4), as well as in murine 2B4.11 T cell hybridoma cell lines stably transfected with the human *bcl-2* gene (not shown). Thus, Bcl-2 fails to neutralize the effects of ICE on mitochondria in vitro, consistent with its inability to prevent ICE-dependent apoptosis in cells. Since Bcl-2 prevents ceramide-induced apoptosis and $\Delta\Psi_m$ disruption (Fig. 1 *C*), we investigated the AIF release of Bcl-2 hyperexpressing mitochondria treated with cytosolic extracts from cells that have been treated during a short interval (30 min) with either ceramide or anti-Fas. Control mitochondria readily release AIF upon incubation with such cytosols (Fig. 5). Bcl-2–hyperexpressing mitochondria demonstrate a selective protection against yet unidentified ceramide-elicited PT inducers, yet release AIF upon incubation with ICE-containing cytosols from anti-Fas–treated cells (Fig. 5). These results are compatible with the hypothesis that Bcl-2 prevents ceramide-induced apoptosis at the level of mitochondria.

AIF Is an Apoptogenic Protease Which Itself Induces PT. AIF is a preformed ~50-kD intermembrane protein that is released from mitochondria undergoing PT (11). Isolated nuclei exposed to AIF exhibit a step-wise alteration in the morphology of the nucleus which consists in a first step of chromatin condensation (15 min), followed by disruption of the nuclear envelope and an associated loss of electron-

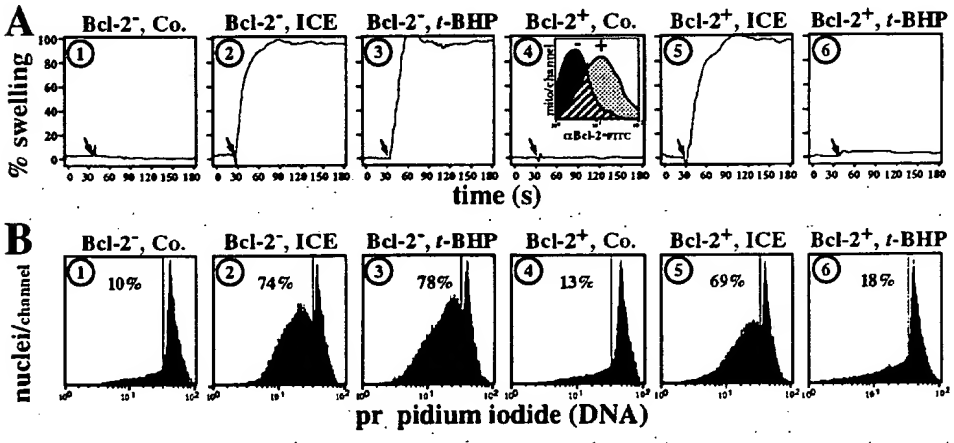

Figure 4. Effect of Bcl-2 hyperexpression on the ICE- or oxidant-induced PT and the release of an AIF from mitochondria. Mitochondria were purified from T cell lymphoma cell lines stably transfected with a human *bcl-2* gene under the control of a tetracyclin-repressable promoter that were treated with doxycyclin (10 ng/ml, 48 h) to repress Bcl-2 expression (Bcl-2⁻, graphs *1–3*), or left untreated (Bcl-2⁺, graphs *4–6*). The inset in graph *4* shows cytofluorometric profiles of isolated mitochondria stained with an anti-hBcl-2-FITC conjugate. These organelles were exposed to CFS buffer only (graphs *1* and *4*) human recombinant ICE (graphs *2* and *5*), or *t*-BHP (graphs *3* and *6*) as described in the legend to Fig. 3, followed by determination of swelling (*A*) and the release of AIF (*B*), which was tested for its capacity to induce hypoploidy in isolated HeLa nuclei. Note that Bcl-2 hyperexpression on the outer mitochondrial membranes does prevent the *t*-BHP–induced PT and AIF release, yet does not affect the ICE-induced PT and AIF release.

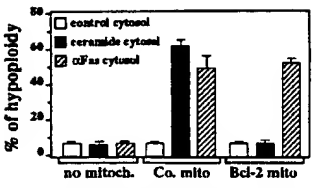

Figure 5. Effect of Bcl-2 on the AIF release triggered by cytosols from ceramide- or Fas-stimulated cells. Cytosols (10^7 cells/100 μl CFS buffer) were prepared from washed (three times) cells which were either left untreated (control) or treated with C_2 ceramide (50 μM) or anti-Fas during 30 min. These cytosols (5 μl) were added to 25 μl CFS buffer only or CFS buffer containing mitochondria (50 μg protein) from control CEM-C7-H2 cells (*Co. mito*) or from Bcl-2–transfected cells (*Bcl-2 mito*), followed by an incubation step of 30 min at 37°C. The supernatants of these cultures (14,000 *g*, 10 min, 4°C) were added to purified HeLa nuclei (3×10^4 nuclei in 10 μl CFS buffer). After 90 min of incubation at 37°C, nuclei were stained with PI and analyzed for the frequency of hypoploid events. One experiment out of two yielding similar results is shown. Independent control experiments indicate that C_2 ceramide itself does not induce PT in isolated mitochondria at a dose up to 50 μM (not shown).

dense material (60 min). At this latter stage, nuclei frequently demonstrate two homogeneous zones that differ in their electron density and resemble nuclei from cells at an advanced stage of apoptosis (Fig. 6 *A*). In addition, isolated nuclei exposed to AIF display two biochemical hallmarks of apoptosis: (*a*) loss of total nuclear DNA (hypoploidy) (11; and Fig. 6 *B*) and (*b*) oligonucleosomal DNA fragmentation (11; and Fig. 6 *C*). The apoptogenic effect of AIF liberated from ICE-treated mitochondria is neutralized by the broad spectrum inhibitor of ICE-like proteases Z-VAD.fmk, but not by the more specific ICE inhibitor Ac-YVAD.cmk (9, 11; and Fig. 6, *B* and *C*), in accord with the fact that ICE itself is not apoptogenic (38), whereas ICE-like proteases do have the capacity to provoke nuclear apoptosis in vitro (41). Since AIF apparently has an ICE-like catalytic activity (11), we tested whether AIF would share with ICE the PT-inducing potential. Indeed, the supernatant of ICE-treated mitochondria provokes PT of freshly isolated mitochondria (Fig. 6 *D*). This activity is not neutralized by Ac-YVAD.cmk, yet is completely abolished by Z-VAD.fmk, suggesting that it is mediated by AIF and not by residual ICE. Accordingly, AIF enriched on an anion exchange FPLC column (11) can induce PT in a Z-VAD.fmk-inhibitable fashion (Fig. 6 *D*). These data suggest that AIF possesses a biological spectrum of activities that overlaps, but is not identical, with that of ICE.

AIF Proteolytically Activates CPP32. The proteolytical activation of CPP32 has been previously shown to be inhibited by Z-VAD.fmk (42), which also inhibits the effects of AIF (11; and Fig. 6). Stimulated by this fact, we have tested whether mitochondrial intermembrane fractions containing AIF would activate purified recombinant CPP32. As shown in Fig. 7 *A*, supernatants of mitochondria induced to undergo PT in response to Atr (9, 11) indeed activate the cleavage of a fluorogeneic peptide substrate containing the CPP32 cleavage site DEVD. This effect is inhibited by Z-VAD.fmk. Moreover, the same effects were observed

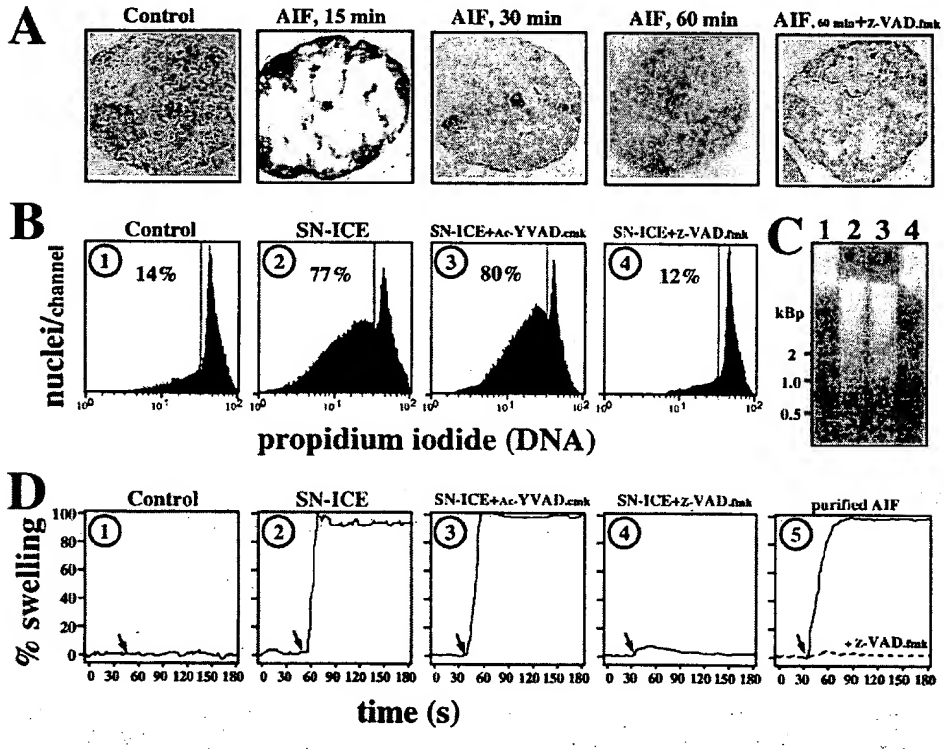

Figure 6. In vitro effects of AIF on isolated nuclei and mitochondria. (*A*) Effect of AIF on nuclear ultrastructure. Isolated HeLa nuclei were incubated with purified AIF (100 ng/ml) and/or the AIF inhibitor Z-VAD.fmk (100 μM) during the indicated interval, followed by transmission electron microscopy. Squares measure 8 μm. (*B* and *C*) ICE triggers the mitochondrial release of AIF. Mitochondria were treated with CFS buffer (*Control*, graph and lane *1*) or recombinant ICE (graphs and lanes *2–4*) in conditions that induce PT (e.g., Figs. 3 and 4), followed by recovery of the mitochondrial supernatant. These supernatants were then tested for their capacity to induce nuclear apoptosis in the absence (graph and lane *2*) or presence of 100 μM Ac.YVAD.cmk (graph and lane *3*) or Z-VAD.fmk (graph and lane *4*). The readout of this system was either the cytofluorometric detection of nuclear hypoploidy (*B*) or agarose electrophores to detect oligonucleosomal DNA fragmentation (*C*) (*D*) Effects of AIF on isolated mitochondria. The same preparations as in *B* and *C* (graphs and lanes *1–4*); were added to purified liver mitochondria, followed by determination of large amplitude swelling. In addition, purified recombinant AIF was tested for its capacity to induce mitochondrial swelling (graph *5*). AIF was either added alone (*solid line*) or together with 100 μM Z-VAD.fmk (*dotted line*), as indicated by the arrow.

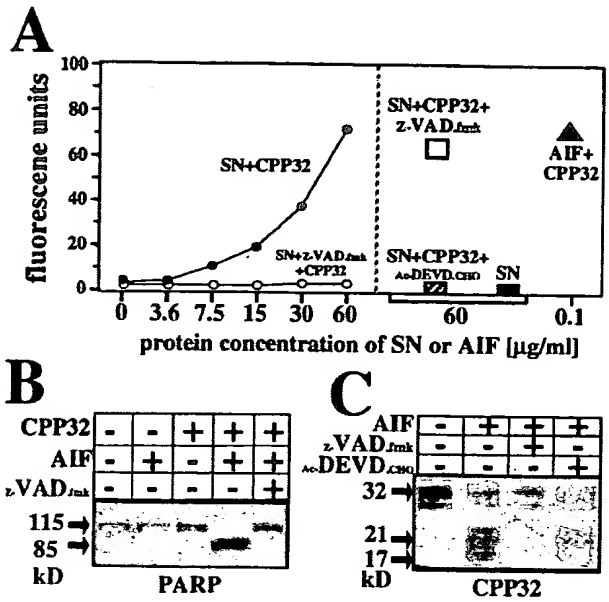

Figure 7. AIF proteolytically activates CPP32. (*A*) Induction of CPP32 activity as determined by a fluorogenic substrate. Variable concentrations of AIF-containing supernatants (*SN*) from Atr-treated mitochondria were added in the presence (*open circles*) or absence of Z-VAD.fmk (100 µM, *filled circles*) to constant amounts (100 ng) of recombinant purified CPP32, followed by determination of the DEVDase activity of CPP32 using the fluorogenic substrate Ac-DEVD-amino-4-methylcoumarin. To exclude that Z-VAD.fmk itself might inhibit the DEVDase activity of CPP32, this inhibitor was added together with the fluorogenic substrate after CPP32 had been activated with SN in the absence of any inhibitor (*open square*). It was also ruled out that the AIF-containing supernatant alone might contain a DEVDase activity (*filled square*). Purified AIF (100 ng/ml) was also used to activate CPP32 (*filled triangle*). (*B*) Induction of CPP32 activity as determined by PARP cleavage. Nuclei were incubated during 90 min at 37°C in the presence or absence of CPP32, AIF-containing supernatant, and/or Z-VAD.fmk, as indicated, followed by Western blotting and immunochemical determination of the cleavage of PARP. Note that only the combination of CPP32 and AIF, but not either of these compounds alone, cause PARP cleavage. (*C*) Proteolysis of CPP32 by AIF. Recombinant CPP32 protein (10 ng) was exposed to the indicated combination of AIF-containing mitochondrial supernatant (10 µg in 50 µl), Z-VAD.fmk (100 µM) and/or Ac-DEVD.CHO (100 µM), followed by Western blot analysis of CPP32 cleavage.

with FPLC-purified AIF (Fig. 7 *A*). In addition, AIF (which is by itself incapable of cleaving the "death substrate" PARP) activates CPP32 to digest PARP (Fig. 7 *B*). As expected by the finding that AIF activates CPP32, CPP32 digestion by AIF-containing preparations yields a 21 precursor and a canonical p17 fragment (Fig. 7 *C*) that may associate with the p12 fragment to yield a biologically active heterotetramer (33, 43). This activation does not require the autocatalytic processing of CPP32, since it is not inhibited by Ac-DEVD.CHO (Fig. 7 *C*). In conclusion, AIF is endowed with the capacity of activating one of the signature processes of apoptosis, CPP32.

Discussion

The data presented in this work provide multiple novel connections between proteases and mitochondrial PT during the apoptotic effector phase. These interactions are bidirectional. On the one hand, ICE can provoke mitochondrial PT, and, on the other hand, PT entails the mitochondrial release of a CPP32-activating protease.

A Novel Pathway of $\Delta\Psi_m$ Disruption: Activation of ICE or ICE-like Proteases. As outlined in the Introduction, $\Delta\Psi_m$ disruption constitutes an early event of apoptosis that precedes nuclear apoptosis. The apoptotic $\Delta\Psi_m$ disruption involves opening PT pores on the inner mitochondrial membrane, based on the observation that PT pore antagonists such as bongkrekic acid inhibit the apoptotic $\Delta\Psi_m$ loss (4, 9, 12). Abundant literature (for review see reference 16) indicates that numerous physiological effectors regulate PT: concentrations of divalent cations and protons, the redox status of mitochondrial thiols (in equilibrium with the redox status of glutathione), the redox status of the pyridine nucleotide pool ($NADH_2$/NAD + $NADPH_2$/NADP; reference 44), concentrations of adenine nucleotides (ADP, ATP), specific peptides, lipid acid oxidation products (16, 45), and proteases from the calpain family (17). Here we show that ICE (or ICE-like proteases) contained in the cytosol of Fas-activated cells, as well as recombinant purified ICE, are capable of inducing a PT-like effect in isolated mitochondria. ICE induces all three hallmarks of PT: (*a*) colloidosmotic swelling (Fig. 3 *A*), (*b*) disruption of the $\Delta\Psi_m$ (Fig. 3 *B*), and (*c*) release of AIF (Fig. 3 *C*), which is self-sufficient to provoke nuclear apoptosis in a cell-free, cytosol-free system. In contrast with other methods of PT induction, ICE-mediated PT is not regulated by various pharmacological inhibitors of PT (e.g., monochlorobiman, bongkrekic acid; Table 1) and it is not inhibited by overexpression of Bcl-2 in the mitochondrial membrane (Fig. 4). Thus, it appears that the direct proteolytic effect of ICE on unidentified mitochondrial substrates provoke PT and a consequent $\Delta\Psi_m$ collapse that disrupts mitochondrial functions. The ICE-induced PT is accompanied by AIF release from mitochondria, similar to PT induced by other compounds including calcium, pro-oxidants, or the thiol–cross-linking agent diamide (9).

It thus emerges that mitochondria function as a cellular sensor of stress including changes in redox potentials, direct oxidative effects, and protease activation. These data support PT as a candidate for the "central apoptotic executioner" that has been postulated by several groups (1–5) and that would allow for the convergence of very different apoptosis induction pathways into one event downstream of which would follow the final common pathway of apoptosis.

A Novel Effector Protease of Mitochondrial Origin, AIF. Irrespective of the PT-triggering stimulus, PT results in the mitochondrial release of an apoptogenic protease that we have termed AIF (9, 11). Although the molecular cloning of cDNA encoding AIF is still in progress, functional tests performed on purified AIF indicate that it possesses three unique features. First, AIF is the first protease that has been shown to suffice in inducing apoptotic changes in isolated nuclei (9, 11; and Fig. 6, *A–C*). Thus, at difference with another mitochondrial product, cytochrome *c* (10), AIF

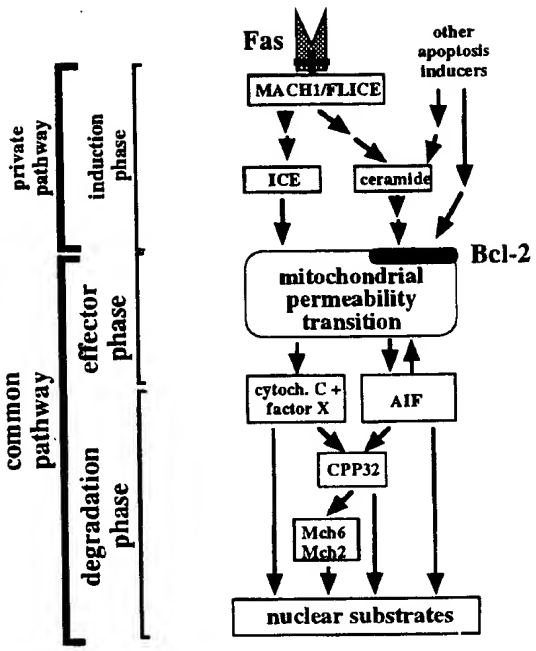

Figure 8. Hypothetical scenario of Fas-induced apoptosis. After trimerization of the Fas receptor and activation of MACH1/FLICE, depending on the cell type, the ceramide and/or the ICE pathways are activated for death induction. Bcl-2 is an efficient inhibitor of ceramide- (and prooxidant-) induced mitochondrial PT, yet fails to prevent the ICE-induced PT. PT marks the initiation of the common effector phase of apoptosis and entails the release of mitochondrial intermembrane proteins including AIF and cytochrome *c*. AIF itself induces PT and thus engages in a self-destructive autoamplification loop. AIF alone and cytochrome *c* in combination with yet unknown cytoplasmic factors are apoptogenic (i.e., cause DNA condensation and fragmentation by acting on nuclear substrates). In addition, they trigger the activation of CPP32 (and possibly, directly or indirectly, of other proteases). For details and references, consult text.

does not appear to require the presence of further cytosolic factors to induce nuclear apoptosis. We cannot exclude the possibility, however, that purified nuclei are associated with factors derived from cytosol that are necessary for AIF function. Second, AIF shares at least one biological effect of ICE, namely the capacity to trigger PT (Fig. 6 *D*). Thus, AIF liberated from mitochondria undergoing PT may engage in a self-amplifying apoptotic switch, and thus aid to lock the cell in an irreversible stage of apoptosis, beyond the point of no return. Since the effects of AIF are inhibited by a degenerate tripeptidic inhibitor of ICE and ICE-like proteases, Z-VAD.fmk (which acts as universal inhibitor of nuclear apoptosis in mammalian cells, perhaps with the exception of blastomeres; references 46, 47), this may explain why Z-VAD.fmk can inhibit $\Delta\Psi_m$ disruption, at least in some systems of apoptosis induction (13). Third, AIF induces cleavage and activation of CPP32 in vitro (Fig. 7). This is a rapid process, with detectable CPP32 cleavage in as little as 5 min (not shown). CPP32 activation appears to be a consistent concomitant of the apoptotic process that may contribute to the apoptotic degradation of different cellular and nuclear substrates (33, 41, 43), including those that are not cleaved by AIF such as PARP (Fig. 7 *B*). This finding is in accord with the fact that the apoptosis-associated activation of CPP32 is inhibited by Z-VAD-fmk in vivo (39, 47). In conclusion, AIF has biological properties which render it a firm candidate to act as a central molecule of the apoptotic effector phase.

A Hypothetical Scenario for Fas-induced Apoptosis. When integrated with the current literature, the data reported in this work suggest the following scenario for Fas-mediated apoptosis (Fig. 8). After Fas cross-linking, the Fas receptor complex rapidly (within seconds) recruits and causes the proteolytic activation of a protease (pro-FLICE/MACH1/Mch5/caspase 8; references 20, 21, 48), which indirectly facilitates the activation of pro-ICE to activate ICE (peak: ~30 min). Thereafter, ICE (or possibly ICE-like proteases) would cause mitochondrial PT (beginning at ~60 min), which in turn would provoke the liberation of AIF from the mitochondrial intermembrane space. AIF then acts as an effector protease or protease activator and activates other downstream enzymes including CPP32. In this scheme, FLICE/MACH1 and ICE would act as "initiator" and "amplifier" proteases (49), within the private initiation phase of Fas-induced apoptosis. ICE and perhaps other ICE-like proteases would then induce mitochondrial PT, a process that causes the release of the "effector" protease/protease activator AIF from mitochondria, which in turn would contribute to further induction of mitochondrial PT. In cells in which Fas-induced apoptosis relies on ICE rather than on other pathways (e.g., ceramide), Bcl-2 would fail to impede the ICE-dependent induction of PT. Thus, PT and associated AIF release would constitute the first event of the common pathway of apoptosis and the central executioner of the effector phase. AIF release then would activate the "machinery" protease (49) CPP32 and perhaps other Ced-3–like proteases, which may participate in the degradation phase of apoptosis.

A possible critique against this sequence of events stems from the evidence that caspases can activate each other via direct interactions, at least in vitro (1–3, 5). Moreover, in some cell-free systems, proteases, in combination with yet unknown cytosolic factors, can provoke nuclear apoptosis (FLICE, ICE, CPP32; references 25, 50). Nonetheless, recombinant caspases including CPP32 do not induce nuclear DNA fragmentation in vitro on their own, in the absence of additional cytoplasmic extracts (33). Moreover, a putative direct caspase activation cascade fails to explain important facts such as the latency between YVADase and DEVDase activation (~2 h) or the temporal sequence between YVADase activation, mitochondrial changes plus CPP32 activation, and late nuclear apoptosis, which is observed in intact cells and is mimicked by our cell-free system. In this context, it may be important to note that cytosolic extracts from cells which have been treated with apoptosis inducers (αFas, ceramide) for a short period (30 min) themselves are inefficient inducers to nuclear apoptosis in vitro, unless mitochondria are added into the system (Fig. 5). Thus, the cell-free system that we are using in this study confirms and extends the notion that mitochondrial

products have a major, and perhaps essential, apoptogenic potential (7–11).

At first glance, our model may appear to be in contradiction with findings reported by Enari et al. (25) who attribute a decisive regulatory role to CPP32 in apoptosis regulation, based on the fact that preincubation of cells with the CPP32 inhibitor Ac-DEVD.CHO prevents Fas-induced apoptosis. However, addition of Ac-DEVD.CHO to cells after Fas cross-linking has no apoptosis-inhibitory effect (25), suggesting that Ac-DEVD.CHO acts on upstream proteases such as caspase 8, which cleaves the sequence motif DEVD (and thus is inhibited by Ac-DEVD.CHO; Reed, J.C., unpublished observation). Thus, the temporal and functional analysis of different proteases activated during Fas-induced apoptosis would suggest that CPP32 participates in the degradation, rather than in the execution, phase of apoptosis. Accordingly, addition of CPP32 inhibitors can suppress detectable DEVDase activation without affecting the mitochondrial phase of the apoptotic process (data not shown). As a caveat, this does not imply that CPP32 (and other closely related Ced-3 homologues) would only participate in the late phase of apoptosis. Indeed, it is conceivable that in response to other apoptosis inducers (e.g., developmentally programmed cell death), CPP32 may be involved in an earlier (private) step of the apoptotic cascade. It has been shown that CPP32 could activate unknown cytosolic factors (25) (which likely include mitochondrial products; reference 10) to become apoptogenic and thus to induce nuclear apoptosis in a cell-free system. These data suggest that CPP32 can activate other, soluble apoptogenic factors.

Irrespective of these possibilities, the results of this work suggest a unified view of protease-dependent and mitochondrial events of the apoptotic cascade. Proteases may have a major impact on mitochondrial function at the same time that mitochondria can release proteases and/or protease activators with apoptosis-inducing properties. The data reported here, therefore, provide new clues about the events that trigger the effector phase of apoptosis.

We thank Anita Diu-Hercend (Roussel Uclaf, Romainville, France) for critical comments and Dr. Maurice Geuskens (Université Libre de Bruxelles, Bruxelles, Belgium) for electron microscopy.

This work was supported by Agence Nationale pour la Recherche contre le SIDA, Association pour la Recherche contre le Cancer, Centre Nationale de la Recherche Scientifique, Fondation de France, Fondation pour la Recherche Médicale/Sidaction, Ligue Française contre le Cancer, Institute National de la Santé et de la Recherche Médicale, North Atlantic Treaty Organization, the French Ministry of Science (to G. Kroemer), and National Institutes of Health grant CA72994 (to J.C. Reed). S.A. Susin receives a postdoctoral fellowship from the European Commission.

Address correspondence to Dr. Guido Kroemer, 19 rue Guy Môquet, B.P. 8, F-94801 Villejuif, France. FAX: 33-1-49-58-35-09.

Received for publication 25 November 1996 and in revised form 19 March 1997.

References

1. Oltvai, Z.N., and S.J. Korsmeyer. 1994. Checkpoints of dueling dimers foil death wishes. *Cell.* 79:189–192.
2. Thompson, C.B. 1995. Apoptosis in the pathogenesis and treatment of disease. *Science (Wash. DC).* 267:1456–1462.
3. Martin, S.J., and D.R. Green. 1995. Protease activation during apoptosis: death by a thousand cuts? *Cell.* 82:349–352.
4. Kroemer, G., P.X. Petit, N. Zamzami, J.-L. Vayssière, and B. Mignotte. 1995. The biochemistry of apoptosis. *FASEB J.* 9: 1277–1287.
5. Henkart, P.A. 1996. ICE family proteases:mediators of all apoptotic cell death? *Immunity.* 4:195–201.
6. Zamzami, N., P. Marchetti, M. Castedo, C. Zanin, J.-L. Vayssière, P.X. Petit, and G. Kroemer. 1995. Reduction in mitochondrial potential constitutes an early irreversible step of programmed lymphocyte death in vivo. *J. Exp. Med.* 181: 1661–1672.
7. Newmeyer, D.D., D.M. Farschon, and J.C. Reed. 1994. Cell-free apoptosis in xenopus egg extracts: inhibition by Bcl-2 and requirement for an organelle fraction enriched in mitochondria. *Cell.* 79:353–364.
8. Martin, S.J., D.D. Newmeyer, S. Mathisa, D.M. Farschon, H.G. Wang, J.C. Reed, R.N. Kolesnick, and D.R. Green. 1995. Cell-free reconstitution of Fas-, UV radiation- and ceramide-induced apoptosis. *EMBO (Eur. Mol. Biol. Organ.) J.* 14:5191–5200.
9. Zamzami, N., S.A. Susin, P. Marchetti, T. Hirsch, I. Gómez-Monterrey, M. Castedo, and G. Kroemer. 1996. Mitochondrial control of nuclear apoptosis. *J. Exp. Med.* 183:1533–1544.
10. Liu, X., C.N. Kim, J. Yang, R. Jemmerson, and X. Wang. 1996. Induction of apoptic program in cell-free extracts: requirement for dATP and cytochrome C. *Cell.* 86:147–157.
11. Susin, S.A., N. Zamzami, M. Castedo, T. Hirsch, P. Marchetti, A. Macho, E. Daugas, M. Geuskens, and G. Kroemer. 1996. Bcl-2 inhibits the mitochondrial release of an apoptogenic protease. *J. Exp. Med.* 184:1331–1342.
12. Zamzami, N., P. Marchetti, M. Castedo, D. Decaudin, A. Macho, T. Hirsch, S.A. Susin, P.X. Petit, B. Mignotte, and G. Kroemer. 1995. Sequential reduction of mitochondrial transmembrane potential and generation of reactive oxygen

species in early programmed cell death. *J. Exp. Med.* 182: 367–377.
13. Marchetti, P., M. Castedo, S.A. Susin, N. Zamzami, T. Hirsch, A. Haeffner, F. Hirsch, M. Geuskens, and G. Kroemer. 1996. Mitochondrial permeability transition is a central coordinating event of apoptosis. *J. Exp. Med.* 184:1155–1160.
14. Crofts, A.R. and J.B. Chappell. 1965. Calcium ion accumulation and volume changes in isolated liver mitochondria. *Biochem. J.* 95:387–392.
15. Castedo, M., T. Hirsch, S.A. Susin, N. Zamzami, P. Marchetti, A. Macho, and G. Kroemer. 1996. Sequential acquisition of mitochondrial and plasma membrane alterations during early lymphocyte apoptosis. *J. Immunol.* 157:512–521.
16. Zoratti, M., and I. Szabò. 1995. The mitochondrial permeability transition. *Biochim. Biophys. Acta.* 1241:139–176.
17. Aguilar, H.I., R. Botla, A.S. Arora, S.F. Bronk, and G.J. Gores. 1996. Induction of the mitochondrial permeability transition by protease activity in rats: a mechanism of hepatocyte necrosis. *Gastroenterology.* 110:558–566.
18. Krammer, P.H., J. Dhein, H. Walczak, I. Behrmann, S. Mariani, B. Matiba, M. Fath, P.T. Daniel, E. Knipping, M.O. Westendorp, et al. 1994. The role of APO-1–mediated apoptosis in the immune system. *Immunol. Rev.* 142:175–191.
19. Nagata, S., and P. Golstein. 1995. The Fas death factor. *Science (Wash. DC).* 267:1449–1456.
20. Boldin, M.P., T.M. Goncharov, Y.V. Goltsev, and D. Wallach. 1996. Involvement of MACH, a novel MORT1/FADD-interacting protease, in Fas/APO- and TNF receptor–induced cell death. *Cell.* 85:803–815.
21. Muzio, M., A.M. Chinnaiyan, F.C. Kischkel, K. O'Rourke, A. Shevchenko, J. Ni, C. Scaffidi, J.D. Bretz, M. Zhang, R. Gentz, et al. 1996. FLICE, a novel FADD-homologous ICE/CED-3–like protease, is recruited to the CD95 (Fas/APO-1) death-inducing signaling complex. *Cell.* 85:817–827.
22. Los, M., M. Van de Craen, L.C. Penning, H. Schenk, M. Westendorp, P.A. Bauerle, W. Dröge, P.H. Krammer, W. Fiers, and K. Schulze-Osthoff. 1995. Requirement of an ICE/CED-3 protease for Fas/Apo-1–mediated apoptose. *Nature (Lond.).* 375:81–83.
23. Enari, M., H. Hug, and S. Nagata. 1995. Involvement of an ICE-like protease in Fas-mediated apoptosis. *Nature (Lond.).* 375:78–81.
24. Kuida, K., J.A. Lippke, G. Ku, M.W. Harding, D.J. Livingston, M.-S. Su, and R.A. Flavell. 1995. Altered cytokine export and apoptosis in mice deficient in interleukin-1β converting enzyme. *Science (Wash. DC).* 267:2000–2003.
25. Enari, M., R.V. Talanian, W.W. Wong, and S. Nagata. 1996. Sequential activation of ICE-like and CPP32-like proteases during Fas-mediated apoptosis. *Nature (Lond.).* 380:723–726.
26. Chiu, V.K., C.M. Walsh, L. Chau-Ching, J.C. Reed, and W.R. Clark. 1995. bcl-2 blocks degranulation but not Fas-based cell-mediated cytotoxicity. *J. Immunol.* 154:2023–2029.
27. Memon, S.A., M.B. Moreno, D. Petrak, and C.M. Zacharchuk. 1995. Bcl-2 blocks glucocorticoid- but not Fas- or activation-induced apoptosis in a T cell hybridoma. *J. Immunol.* 155:4644–4652.
28. Strasser, A., A.W. Harris, D.C.S. Huang, P.H. Krammer, and S. Cory. 1995. Bcl-2 and Fas/APO-1 regulate distinct pathways to lymphocyte apoptosis. *EMBO (Eur. Mol. Biol. Organ.) J.* 14:6136–6147.
29. Gossen, M., and H. Bujard. 1992. Tight control of gene expression in mammalian cells by tetracycline responsive promoters. *Proc. Natl. Acad. Sci. USA.* 89:5547–5551.
30. Yin, D.X., and R.T. Schimke. 1995. BCL-2 expression delays drug-induced apoptosis but does not increase clonogenic survival after drug treatment in HeLa cells. *Cancer Res.* 55: 4922–4928.
31. Macho, A., D. Decaudin, M. Castedo, T. Hirsch, S.A. Susin, N. Zamzami, and G. Kroemer. 1996. Chloromethyl-X-rosamine is an aldehyde-fixable potential-sensitive fluorochrome for the detection of early apoptosis. *Cytometry.* 25:333–340.
32. Enari, M., A. Hase, and S. Nagata. 1995. Apoptosis by a cytosolic extract from Fas-activated cells. *EMBO (Eur. Mol. Biol. Organ.) J.* 14:5201–5208.
33. Nicholson, D.W., A. Ali, N.A. Thornberry, J.P. Vaillancourt, C.K. Ding, M. Gallant, Y. Gareau, P.R. Griffin, M. Labelle, Y.A. Lazebnik, et al. 1995. Identification and inhibition of the ICE/CED-3 protease necessary for mammalian apoptosis. *Nature (Lond.).* 376:37–43.
34. Petit, P.X., J.E. O'Connor, D. Grunwald, and S.C. Brown. 1990. Analysis of the membrane potential of rat- and mouse-liver mitochondria by flow cytometry and possible applications. *Eur. J. Biochem.* 220:389–397.
35. Lazebnik, Y.A., S. Cole, C.A. Cooke, W.G. Nelson, and W.C. Earnshaw. 1993. Nuclear events of apoptosis in vitro in cell-free mitotic extracts: a model system for analysis of the active phase of apoptosis. *J. Cell Biol.* 123:7–22.
36. Miossec, C., M.C. Decoen, L. Durand, F. Fassy, and A. Diu-Hercend. 1996. Use of monoclonal antibodies to study interleukin-1β converting enzyme expression: only precursor forms are detected in interleukin-1β secreting cells. *Eur. J. Immunol.* 26:1032–1042.
37. Macho, A., Z. Mishal, and J. Uriel. 1996. Molar quantification by flow cytometry of fatty acid binding to cells using dipyrrometheneboron difluoride derivatives. *Cytometry.* 23: 166–173.
38. Lazebnik, Y.A., S.H. Kaufmann, S. Desnoyers, G.G. Poirier, and W.C. Earnshaw. 1994. Cleavage of poly(ADP-ribose) polymerase by a proteinase with properties like ICE. *Nature (Lond.).* 371:346–347.
39. Chinnaiyan, A.M., K. Orth, K. O'Rourke, H.J. Duan, G.G. Poirier, and V.M. Dixit. 1996. Molecular ordering of the cell death pathway: Bcl-2 and Bcl-X(L) function upstream of the CED-3–like apoptotic proteases. *J. Biol. Chem.* 271:4573–4576.
40. Williams, M.S., and P.A. Henkart. 1994. Apoptotic cell death induced by intracellular proteolysis. *J. Immunol.* 153:4247–4255.
41. Lazebnik, Y.a., A. Takayashi, R.D. Moir, R.D. Goldman, G.G. Poirier, S.H. Kaufmann, and W.C. Earnshaw. 1995. Studies of the lamin proteinase reveal multiple parallel biochemical pathways during apoptotic execution. *Proc. Natl. Acad. Sci. USA.* 92:9042–9046.
42. Slee, E.A., H.J. Zhu, S.C. Chow, M. Macfarlane, D.W. Nicholson, and G.M. Cohen. 1996. Benzyloxycarbonyl-Val-Ala-Asp (OMe) fluoromethylketone (Z-VAD.fmk) inhibits apoptosis by blocking the processing of CPP32. *Biochem. J.* 315:21–24.
43. Tewari, M., L.T. Quan, K. O'Rourke, S. Desnoyers, Z. Zeng, D.R. Beidler, G.G. Poirier, G.S. Salvesen, and V.M. Dixit. 1995. Yama/CPP32 beta, a mammalian homolog of CED-3, is a CrmA-inhibitable protease that cleaves the death substrate poly(ADP-ribose) polymerase. *Cell.* 81:801–809.
44. Costantini, P., B.V. Chernyak, V. Petronilli, and P. Bernardi. 1996. Modulation of the mitochondrial permeability transition pore by pyridine nucleotides and dithiol oxidation at

two separate sites. *J. Biol. Chem.* 271:6746–6751.
45. Kirstal, B.S., B.K. Park, and B.P. Yu. 1996. 4-Hydroxyhexenal is a potent inducer of the mitochondrial permeability transition. *J. Biol. Chem.* 271:6033–6038.
46. Zhivotovsky, B., A. Gahm, M. Ankarcrona, P. Nicotera, and S. Orrenius. 1995. Multiple proteases are involved in thymocyte apoptosis. *Exp. Cell Res.* 221:404–412.
47. Jacobson, M.D., M. Weil, and M.C. Raff. 1996. Role of Ced-3/ICE-family proteases in staurosporine-induced programmed cell death. *J Cell Biol.* 133:1041–1051.
48. Fernandes-Alnemri, T., R.C. Armstrong, J. Krebs, S.M. Srinivasula, L. Wang, F. Bullrich, L.C. Fritz, J.A. Trapani, K.J. Tomaselli, G. Litwack, and E.S. Alnemri. 1996. In vitro activation of CPP32 and Mch3 by Mch4, a novel human apoptotic cysteine protease containing two FADD-like domains. *Proc. Natl. Acad. Sci. USA.* 93:7464–7469.
49. Fraser, A., and G. Evan. 1996. A license to kill. *Cell.* 85: 781–784.
50. Muzio, M., G.S. Salvesen, and V.M. Dixit. 1997. FLICE induced apoptosis in a cell-free system. Cleavage of caspase zymogens. *J. Biol. Chem.* 272:2952–2956.